

Experimental validation of Time Optimal MPC on a flexible motion system

Lieboud Van den Broeck, Moritz Diehl and Jan Swevers

Abstract—This paper discusses the application and experimental validation of time-optimal model predictive control (TOMPC) on a flexible motion system, an overhead crane with fixed cable length. TOMPC realizes minimal settling times for point-to-point motions taking into account system constraints. Results of several different point-to-point motion experiments and of disturbance rejection experiments clearly demonstrate this time optimal behavior. The extension of the TOMPC algorithm to increase its feasibility range required for large point-to-point motions is discussed and validated.

I. INTRODUCTION

In order to control the point-to-point motion of flexible mechatronic systems, usually linear feedback control [1], [2] is combined with reference trajectories. Feedback provides the system input by comparing the output with the reference trajectory and takes care of disturbances that occur during motion and positioning. The reference trajectory is designed such that the requested point-to-point motion is realized according to specifications while respecting the actuator constraints. Different approaches for this reference generation are possible. One approach computes the reference trajectories beforehand and thereby optimizes the performance (e.g. time duration) for one specific point-to-point motion [3], [4], taking into account the system constraints. Other approaches like inputshaping [5]–[7] filter an applied reference step on-line, thereby transforming this step into a more suitable reference trajectory which satisfies all system constraints for the largest possible reference step. The main drawback of these approaches occur when many different steps over a wide range are requested. These approaches require then either a large number of precomputed trajectories or are too conservative for all reference steps except the largest one. For these applications, model predictive control (MPC) [8],

[9] is a better alternative. This type of controllers computes on-line during the motion the optimal input by solving an optimization problem over a given prediction horizon, taking the actuator constraints and the current state of the system explicitly into account, thereby allowing constraint satisfaction for every possible point-to-point motion and incorporating feedback. The first part of the optimized input is applied to the system and then this procedure is repeated every sampling time over a shifted horizon. The main drawback of MPC is the high computational load that stems from the optimization and which depends on the number of variables and hence the length of the prediction horizon and the order of the considered system.

MPC became very popular in the eighties [10], mostly for process control applications which have less stringent real-time requirements due to low sampling rates in the order of seconds or minutes [11]. Since the end of the nineties, much research has been dedicated towards the development of fast solution methods for MPC (fast MPC in short) to extend its application area to faster systems such as mechatronic systems. One fast MPC approach, called explicit MPC [12], [13], stores exact precomputed optimal control solutions, depending on the current state. This approach is successfully applied to numerous control problems, however the system dimensions and prediction horizon are typically limited to 5 each, due to storage requirements and a too complex search space. In order to avoid these limitations, other fast MPC approaches use fast numerical solution methods as qpOASES [14] to solve the optimal control problem in real-time. This approach is applied to systems with up to 10-20 states and prediction horizons of 10-12 time-steps at kHz sampling rates [15], [16].

In order to control the transient behavior between two setpoints, MPC typically optimizes a least squares objective function weighting the input cost against the response speed. However, for most mechatronic applications, the input cost is negligible and time optimality is the main goal. Hence the need for an MPC formulation that aims at time optimal system control, i.e. achieving a minimal settling time while respecting the system constraints. Although time optimality is requested for completing a point-to-point motion, this dead beat behavior is not desirable when the system reacts on measurement noise. Therefore, the time optimal behavior has to be combined with local quadratic cost function behavior, typical for traditional MPC, in order to reduce the sensitivity to measurement noise close to the setpoint. This paper applies a scheme addressing both requirements, called Time Optimal MPC (TOMPC) [17], [18]. This paper extends the

Lieboud Van den Broeck is funded by a Ph.D. fellowship of the Research Foundation - Flanders (FWO - Vlaanderen). This work benefits from K.U.Leuven-BOF PFV/10/002 Center-of-Excellence Optimization in Engineering (OPTEC), the Belgian Programme on Interuniversity Attraction Poles, initiated by the Belgian Federal Science Policy Office (DYSCO), research project FP7-HD-MPC, research project EMBOCOM FP7-ICT-2009-4 248940, research project IWT-SBO 80032 (LeCoPro) of the Institute for the Promotion of Innovation through Science and Technology in Flanders (IWT-Vlaanderen), research project G.0422.08 of the Research Foundation - Flanders (FWO -Vlaanderen), and K.U.Leuven's Concerted Research Action GOA/10/11 Global real-time optimal control of autonomous robots and mechatronic systems. The research leading to these results has received funding from the European Union Seventh Framework Programme FP7/2007-2013 under grant agreement number FP7-ICT-2009-4 248940.

L. Van den Broeck and J.Swevers are with the Department of Mechanical Engineering, division PMA, K.U.Leuven, 3001 Leuven, Belgium lieboud.vandenbroeck@mech.kuleuven.be

M. Diehl is with the Department of Electrical Engineering, K.U.Leuven, 3001 Leuven, Belgium

basic TOMPC approach to allow for longer horizons and hence larger reference steps and applies the controller to an overhead crane with constant cable length. This system is of higher order than the system considered in previous applications of TOMPC [17], [18].

The paper is organized as follows. Section II presents the idea of TOMPC, and shows how the problem can efficiently be solved. Moreover, it is shown how the attainable range of the controller is extended. Section III discusses and validates the implementation of TOMPC on an overhead crane in detail. Section IV concludes the paper.

II. TOMPC

This section describes the applied TOMPC technique. First, the basic TOMPC optimization problem is introduced. Second, it is shown how this optimization problem can be solved efficiently. Finally, the extension to allow longer horizons and hence larger reference steps is discussed.

A. Basic technique

This paragraph briefly discusses the basic idea of Time Optimal MPC (TOMPC). A more comprehensive explanation can be found in [17].

First, a traditional MPC problem (1) with horizon N is defined as problem $P_A(\bar{x}_l, N)$, thereby explicitly stressing the problem's dependence on the current state \bar{x}_l and the length of the horizon N . $P_A(\bar{x}_l, N)$:

$$V_A^*(\bar{x}_l, N) = \min_{x_0, \dots, x_N, u_0, \dots, u_{N-1}} \sum_{k=0}^{N-1} \|u_k - u_{\text{ref}}\|_R^2 + \|x_k - x_{\text{ref}}\|_Q^2, \quad (1a)$$

subject to the constraints:

$$x_0 = \bar{x}_l, \quad (1b)$$

$$x_{k+1} = Ax_k + Bu_k, \quad (1c)$$

$$Hx_k + Gu_k \geq e \quad k \in [0, N-1], \quad (1d)$$

$$x_N = x_{\text{ref}}, \quad (1e)$$

where goal function (1a) makes a trade-off between the input cost and the output error, (1b) constrains the system state at the beginning of the prediction horizon x_0 to be equal to the estimated current system state \bar{x}_l , constraint (1c) imposes the system model, constraint (1d) imposes the system constraints and constraint (1e) requires the system to be at rest at the reference position at time N expressed by the reference state x_{ref} . Function V_A^* is extended to $V_A^* = \infty$ if $P_A(\bar{x}_l, N)$ is infeasible, i.e. the system can not settle at x_{ref} at time N while respecting all constraints (1d). This allows us to define a feasible set of initial system states from which the reference state x_{ref} can be reached within N time steps:

$$\mathbb{X}(N) = \{\bar{x}_l | V_A^*(\bar{x}_l, N) \text{ is finite.}\} \quad (2)$$

Second, a mixed integer optimization problem $P_B(\bar{x}_l)$ is defined:

$$V_B^*(\bar{x}_l) = \min_{N \in \mathbb{N}} N \quad (3a)$$

subject to the constraints:

$$N \geq N_{\min}, \quad (3b)$$

$$N \leq N_{\max}, \quad (3c)$$

$$\bar{x}_l \in \mathbb{X}(N), \quad (3d)$$

where N is the settling time as defined above, N_{\max} is the maximal optimization horizon and N_{\min} is a minimal bound on N . The optimization problem hence consists of two parts. First problem P_B is optimized, minimizing the required time N to settle. Traditional MPC problem P_A is optimized, if additional optimization freedom is left, i.e. if $N = N_{\min}$ or if multiple time optimal solutions exist. The choice of N_{\min} allows us a trade-off between time-optimality and sensitivity to measurement noise [18].

B. Efficient real-time solution

To solve mixed integer problem P_B in real-time, it is useful to remark that this problem is quasi-convex, i.e. if the problem is feasible for $N = N_1$ it is also feasible for $N = N_2 > N_1$. Therefore, problem P_B is solved by a series of feasibility problems P_A , thereby increasing or decreasing the guess of optimal N by one, assuming that a good initial guess is available. To solve the total optimization problem P_B in real-time for a mechatronic system, i.e. within a sampling period which is of the order of magnitude of milliseconds, problem P_A is first reformulated into a problem of constant size, such that an efficient online active set approach [16] can be applied. Therefore, the variables of problem P_A are extended to $(x_0, \dots, x_{N_{\max}})$ and $(u_0, \dots, u_{N_{\max}-1})$, irrespective of the value N , and extra constraints are added to optimization problem (1):

$$u_k = u_{\text{ref}} \text{ for } k = N, \dots, N_{\max}-1. \quad (4)$$

In order to further exploit the problem structure, the problem is further extended with the variables $(u_{N_{\max}}, \dots, u_{N_{\max}+n-2})$ and $(x_{N_{\max}+1}, \dots, x_{N_{\max}+n-1})$, and endpoint constraint (1e) is replaced by:

$$y_{N+k} = y_{\text{ref}} \text{ for } k = 0, \dots, n-1, \quad (5)$$

where $y_k = Cx_k + Du_k$ is the system output at time k , y_{ref} is the reference position and n the system order. This reformulation can be shown to be equivalent to (1e) if the observability matrix of the system is of full rank. This reformulation allows for a more efficient shifting of the active set constraints between subsequent feasibility problems. Remark that this second extension again yields sets of optimization variables of constant size such that the efficient active set approach [16] can still be used. The combination of these reformulations reduces the worst case computation time, i.e. the highest required computation time typically necessary when a new reference step is requested, with a factor of 7.5 as shown in [19].

C. Extension for longer horizon

With the above described TOMPC algorithm, the largest possible reference step depends on the value of N_{\max} because end point constraints (1e) and (4) must be satisfied for $N \leq N_{\max}$, that is, the system must be able to reach this largest possible reference position in no more than N_{\max} time steps without violating the system constraints (1d). N_{\max} itself determines the size of the optimization problem and hence the worst case computation time of the TOMPC solution method which is limited by the sampling period. Hence, the sampling period limits the largest possible reference step, which can be small for systems that require high sampling frequencies. In order to overcome this limitation, non-equidistant time steps or time gridding is applied such that larger horizons can be considered without increasing the total number of discretization points N_{\max} and optimization variables. In the first part of the horizon up to typically N_{\min} , the time step corresponds to the sampling period. Thereafter, the time steps are gradually increased up to 10 times the sampling time in order to have a larger prediction horizon and therefore a larger feasible set of reference steps. For the overhead crane test setup of Section III this allows us to increase the prediction horizon by a factor of 4, extending the attainable range to its maximum of 70cm.

III. EXPERIMENTAL VALIDATION

This section discusses the implementation and experimental validation of TOMPC on an overhead crane with fixed cable length, a typical example of an linear time invariant mechatronic system.

A. Test setup

The considered test setup is the overhead crane with fixed cable length shown in Fig. 1. Fig. 2 shows a schematic representation of this system. The actuator of the system is a velocity controlled DC-motor that drives a trolley through a rack and pinion. The position of the trolley x is measured using an angular encoder mounted on the DC-motor axle, yielding a position measurement resolution of $3\mu\text{m}$. The swing angle θ is measured using a rotative encoder mounted on the axle to which the cable is attached, yielding an angular resolution of 0.0009° . The input to this system is a voltage u , which is a reference applied to the 25Hz bandwidth internal velocity loop. The input is limited to $\pm 1\text{V}$ and the input slew rate is limited to $\pm 6\text{V/s}$ due to limitations of the motor current amplifier. The maximal range of the trolley is 70cm. The length of the cable is fixed to 450mm. The system controllers are embedded on a dSPACE board DS1103 and implemented through C++-functions in the real-time-target environment of Simulink. The system controllers are applied at a sampling frequency of 60Hz.

The relation between the input u and the position of the trolley x is modelled by a first order model for the internal velocity loop in combination with an integrator relating velocity to position:

$$\frac{X(s)}{U(s)} = \frac{K}{s(s-a)}. \quad (6)$$

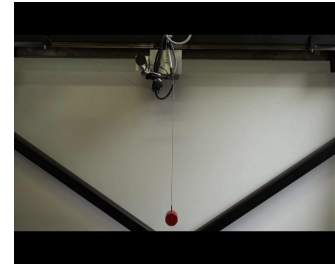


Fig. 1. The overhead crane in the PMA-lab at K.U.Leuven.

The relation between the position of the trolley x and swing angle θ can for small values of θ be modelled as [20]:

$$\frac{\theta(s)}{X(s)} = \frac{s^2}{Ls^2 + g}, \quad (7)$$

with L the length of the cable and g the gravitational acceleration. These models (6)–(7) are combined and discretized, to yield following discrete time models:

$$\frac{X(z)}{U(z)} = \frac{b_0 z}{(z-1)(z-a_0)}, \quad (8a)$$

$$\frac{\theta(z)}{U(z)} = \frac{\beta_0 z(z-1)}{(z^2 + \alpha_1 z + \alpha_2)(z-a_0)}. \quad (8b)$$

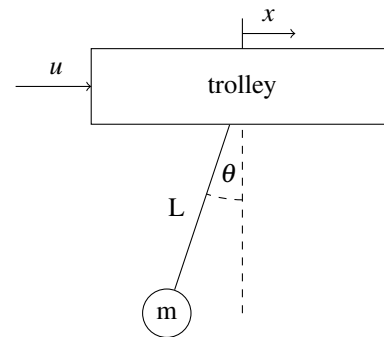


Fig. 2. Schematic representation of the overhead crane

The parameters of models (8a)–(8b) are identified using a nonlinear least square frequency domain identification approach based on frequency response function (FRF) measurements that are obtained from multisine excitations with a frequency content between 0.05Hz and 5Hz [21]. Fig. 3 shows the results of this identification, that is, a good fit between the measured FRF's (black) and the FRF's of the two identified models (grey). The estimated resonance frequency is 0.74Hz which corresponds to the theoretical value $\frac{1}{2\pi} \sqrt{\frac{g}{L}}$ with $L = 450\text{mm}$. The damping of the estimated resonance frequency is $\zeta = 0.00168$ which is extremely low.

The two identified models are then combined into the

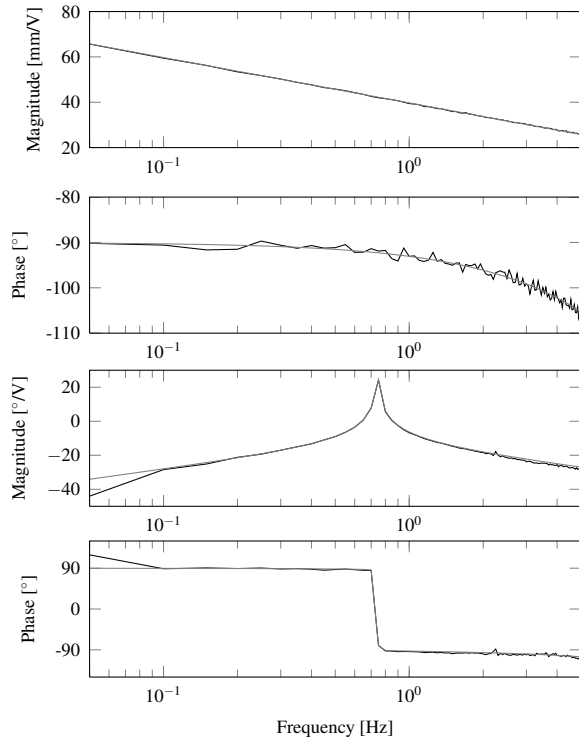


Fig. 3. Measured FRF (black) and FRF of the identified models (grey). The upper 2 plots show the bode plot from input u to position of the trolley x and the lower 2 plots show the bode plot from u to swing angle θ .

following discrete time fourth order state space model:

$$A = \begin{bmatrix} 0.996 & 4.35E-3 & 0 & 0 \\ 1 & 0 & 0 & 0 \\ 0.0438 & -0.0438 & 1.99 & -0.9997 \\ 0 & 0 & 1 & 0 \end{bmatrix}, D = \begin{bmatrix} 0 \\ 0 \\ 0 \\ 0 \end{bmatrix},$$

$$B = \begin{bmatrix} -826.1 \\ 0 \\ 35.99 \\ 0 \end{bmatrix}, C = \begin{bmatrix} -0.0122 & 0 & 0 & 0 \\ 0 & 0 & 0.036 & 0 \\ -0.0122 & 0 & 0.2827 & 0 \end{bmatrix}. \quad (9)$$

The first output of the system is the position of the trolley x and the second output is the swing angle θ . The third output is the position of the load $y = x + L\theta \frac{\pi}{180}$ in mm. This expression is valid assuming small values of θ .

B. TOMPC controller

For this system, a TOMPC controller is developed taking into account the abovementioned constraints on input and input slew rate. As the states of model (9) are not directly measurable, first a Luenberger observer [22] is designed. For the estimation of the states, the measurements of both the position of the trolley x and the swing angle θ are used. The best results are obtained using a state observer with a bandwidth of 0.95Hz. Higher observer bandwidths yield a too nervous or even unstable behavior. As the solution of optimization problem (3) requires a large computation time, the control input is only available near the end of every sample period, and this introduces an additional delay. To

account for this delay, the state space model is extended with one delay state, resulting in the following new state space matrices:

$$A' = \begin{bmatrix} A & B \\ 0 & 0 \end{bmatrix}, \quad B' = \begin{bmatrix} 0 \\ 1 \end{bmatrix},$$

$$C' = [C(3) \quad D(3)], \quad D' = 0$$

where $C(3)$ and $D(3)$ denote the third row of C and D (9) respectively, since the output considered in end point constraint (5) of the TOMPC implementation, is the position of the lower mass. Based on this fifth order model, the TOMPC is implemented. Fig. 4 and 5 show the response of the system with TOMPC on a reference step of 10cm. Fig. 6 shows the corresponding input to the system. The constraints on the input amplitude are not reached. The input slew rate however, shown in Fig. 7, reaches the slew rate constraints during almost the whole duration of the motion. This shows that the system is working at its limits and hence that the controller steers the system as fast as possible to the desired endpoint.

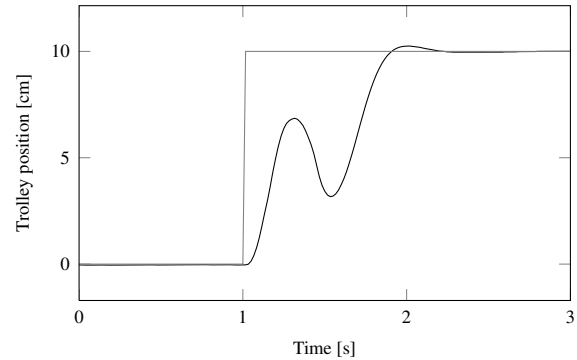


Fig. 4. Position of the trolley (black) controlled by a TOMPC controller for a reference step of 10cm (grey).

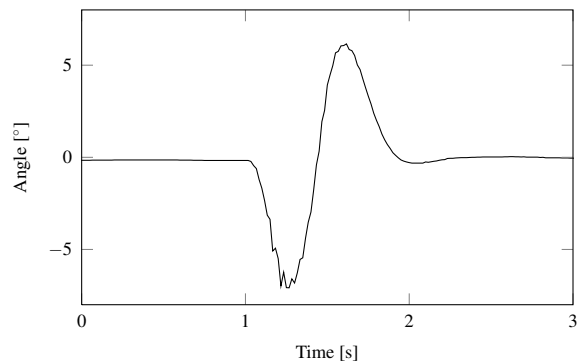


Fig. 5. Swing angle of the TOMPC controlled system for a reference step of 10cm.

A similar time optimal behavior can also be attained using an optimized reference trajectory (e.g. [3]) and a linear controller. However with the linear controller approach, time optimality can only be obtained if for each possible reference step a new reference trajectory optimization is

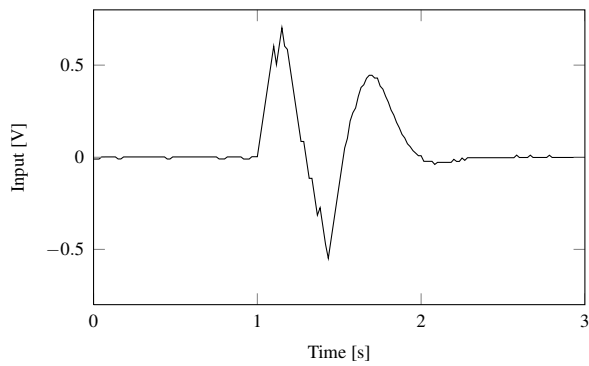


Fig. 6. Input applied to the overhead crane for a requested step of 10cm controlled by a TOMPC controller.

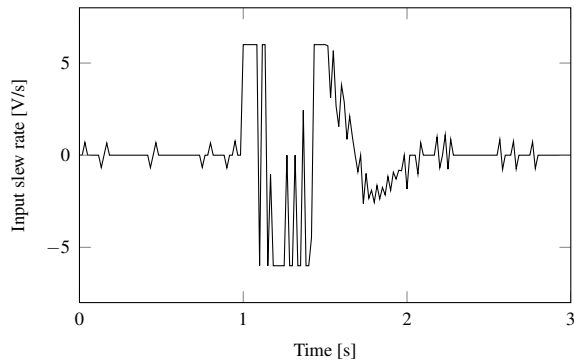


Fig. 7. Differential input applied to the overhead crane for a requested step of 10cm controlled by a TOMPC controller.

performed, while the presented TOMPC obtains this behavior for all possible references. This is illustrated in the following figures. Figs. 8, 9 and 10 show respectively the position of the trolley x , the swing angle θ and the input u for several reference steps ranging from 20cm to 50cm. Fig. 10 and more clearly Fig. 11 show that the controller is continuously hitting the input constraints during the motion, showing its time optimality for all reference steps.

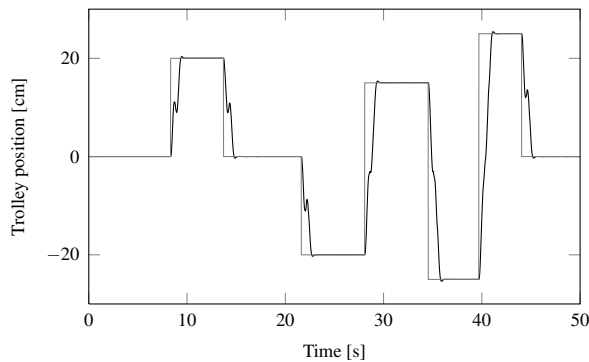


Fig. 8. Position of the trolley (black) controlled by a TOMPC controller for a series of reference steps (grey).

A last set of experiments illustrates the TOMPC controller disturbance rejection capabilities. Fig. 12 shows the position of the trolley x and Fig. 13 the swing angle θ when an

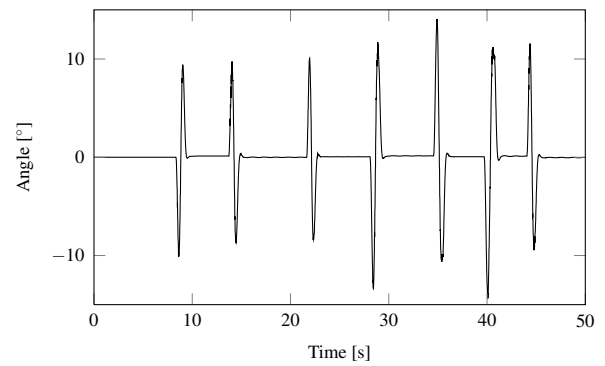


Fig. 9. Swing angle of the TOMPC controlled system for a series of reference steps.

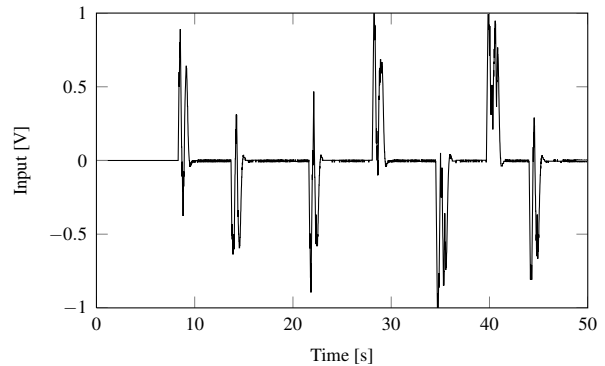


Fig. 10. Input applied to the overhead crane controlled by a TOMPC controller for a series of reference steps.

external disturbance is applied to the lower mass. From time 1.2s till 1.5s, as indicated by a grey zone in Fig. 13, the lower mass is manually moved out of its equilibrium position $\theta = 0$ and is released at time 1.5s. The controller reacts to this disturbance, and steers the system in minimal time back to its desired zero position. Fig. 14 illustrates the time optimality of the reaction to disturbances by showing the input slew rate, which is again hitting continuously the slew rate constraints.

IV. CONCLUSION

A time optimal MPC approach is successfully applied to a flexible motion system. The basic time optimal MPC approach is first adapted to extend the feasible range of the controller without compromising on the corresponding computational load and sampling time. This MPC controller steers the system to the desired setpoint and regulates disturbances in a minimal time. This minimal time depends on the size of the reference step and disturbance and on the system input and input slew rate constraints.

REFERENCES

- [1] T. Zhou, J. Doyle, and K. Glover. *Robust and Optimal Control*. Prentice Hall, 1995.
- [2] G.F. Franklin, D.J. Powell, and A. Emami-Naeini. *Feedback Control of Dynamic Systems*. Prentice Hall PTR, 2001.

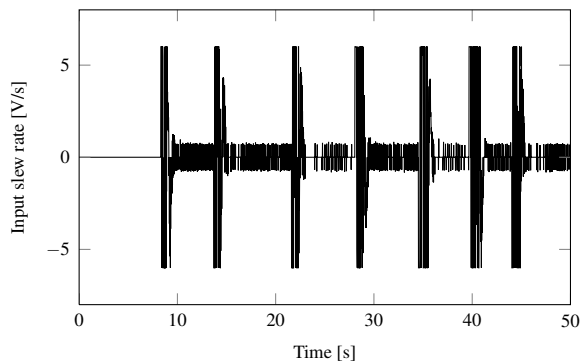


Fig. 11. Differential input applied to the overhead crane controlled by a TOMPC controller for a series of reference steps.

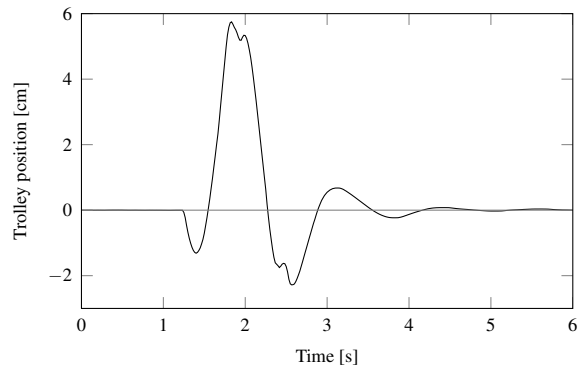


Fig. 12. Position of the trolley (black) controlled around the zero position (grey) by a TOMPC controller when a disturbance is applied.

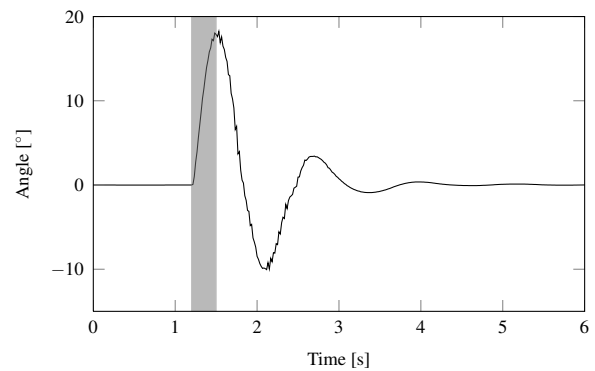


Fig. 13. Swing angle of the TOMPC controlled system when a disturbance is applied.

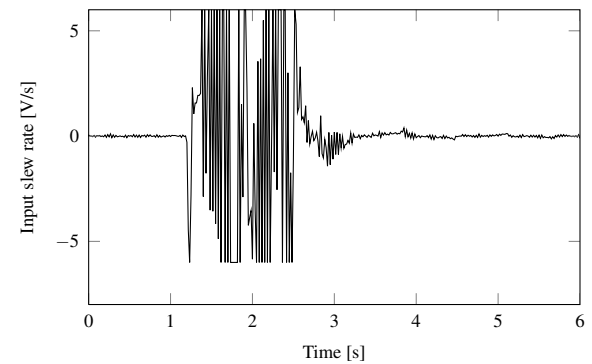


Fig. 14. Differential input applied to the overhead crane controlled by a TOMPC controller when a disturbance is applied.

- [3] B. Demeulenaere, J. De Caigny, G. Pipeleers, J. De Schutter, and J. Swevers. Optimal splines for rigid motion systems: benchmarking and extensions. *Transactions of the ASME, Journal of Mechanical Design*, 131, 2009. In press.
- [4] P. Lambrechts, M. Boerlage, and M. Steinbuch. Trajectory planning and feedforward design for electromechanical motion systems. *Control Engineering Practice*, 13(2):145 – 157, 2005.
- [5] N. C. Singer and W. P. Seering. Preshaping command inputs to reduce system vibration. *Transactions of the ASME, Journal of Dynamic Systems, Measurement, and Control*, 112:76–82, 1990.
- [6] W.E. Singhose, W. P. Seering, and N.C. Singer. Time-optimal negative input shapers. *Journal of Dynamic Systems Measurement and Control-Transactions of the ASME*, 119:198–205, 1997.
- [7] M. D. Baumgart and L. Y. Pao. Discrete time-optimal command shaping. *Automatica*, 43:1403–1409, 2007.
- [8] J.M. Maciejowski. *Predictive control with constraints*. Prentice Hall, 2000.
- [9] JB Rawlings. Tutorial overview of model predictive control. *IEEE Control Systems Magazine*, 20(3):38–52, JUN 2000.
- [10] C.E. García, D.M. Prett, and M. Morari. Model Predictive Control: Theory and Practice – a Survey. *Automatica*, 25:335ff, 1989.
- [11] S.J. Qin and T.A. Badgwell. A survey of industrial model predictive control technology. *Control Engineering Practice*, 11:733–764, 2003.
- [12] A. Bemporad, M. Morari, V. Dua, and E.N. Pistikopoulos. The explicit linear quadratic regulator for constrained systems. *Automatica*, 38:3–20, 2002.
- [13] A. Bemporad, F. Borrelli, and M. Morari. Model predictive control based on linear programming the explicit solution. *Automatic Control, IEEE Transactions on*, 47(12):1974 – 1985, dec. 2002.
- [14] H.J. Ferreau, H.G. Bock, and M. Diehl. An online active set strategy to overcome the limitations of explicit mpc. *International Journal of Robust and Nonlinear Control*, 18(8):816–830, 2008.
- [15] A.G. Wills, D. Bates, A.J. Fleming, B. Ninness, and S.O.R. Moheimani. Application of mpc to an active structure using sampling rates up to 25khz. In *Proceedings of the Conference on Decision and Control and European Control Conference ECC'05*, Seville, 2005.
- [16] H.J. Ferreau, P. Ortner, P. Langthaler, L. del Re, and M. Diehl. Predictive control of a real-world diesel engine using an extended online active set strategy. *Annual Reviews in Control*, 31(2):293–301, 2007.
- [17] L. Van den Broeck, M. Diehl, and J. Swevers. Time optimal MPC for mechatronic applications. In *Proceedings of the 48th IEEE Conference on Decision and Control*, Shanghai, 16-18 December 2009.
- [18] L. Van den Broeck, J. Swevers, and M. Diehl. Experimental validation of time optimal MPC on a linear drive system. In *Proceedings of the 11th International Workshop on Advanced Motion Control*, pages 355–360. Nagaoka, Japan, 2010.
- [19] L. Van den Broeck. Time optimal model predictive control and its fast computation for motion control of mechatronic systems. Technical report, K.U.Leuven, 2010.
- [20] M. Fliess, J. Levine, P. Martin, and P. Rouchon. Flatness and defect of nonlinear systems: Introductory theory and examples. Technical report, CAS, 1994.
- [21] R. Pintelon and J. Schoukens. *System Identification: A Frequency Domain Approach*. IEEE Press, 2001.
- [22] D.G. Luenberger. Introduction To Observers. *Ieee Transactions On Automatic Control*, AC16(6):596–602, 1971.